13th Int. Particle Acc. Conf. IPAC2022, Bangkok, Thailand JACoW Publishing
ISBN: 978-3-95450-227-1 ISSN: 2673-5490 doi:10.18429/JACoW-IPAC2022-MOPOTK009

BASIC DESIGN CHOICES FOR THE BESSY III MBA LATTICE *

B. C. Kuske†, M. Abo-Bakr, P. Goslawski, Helmholtz-Zentrum Berlin, 12489 Berlin, Germany

Abstract

Lattice development for the 2.5 GeV, low emittance successor of BESSY II, are ongoing at HZB since 2 years, [1]. The choice of a multi-bend achromat lattice is indispensable due to the emittance goal of 100 pm, required to generate diffraction limited radiation up to 1 keV. Hard boundary conditions for the design are a relatively short circumference of ≈ 350 m due to the accessible construction property in vicinity to Bessy II and 16 super-periods to not step behind the number of existing experimental stations. The configuration of the two building blocks of MBA lattices - unit cell and dispersion suppression cell - has been thoroughly studied from basic principles. It was found that gradient free bending dipoles are the better choice for the BESSY III lattice, opposite to the concepts of comparable projects.

INTRODUCTION

Since the successful operation of MAX IV in Lund, Sweden [2], the innovative idea of multi-bend achromat (MBA) lattices entered basically every new low emittance storage ring design. In 2014, A. Streun, PSI, analysed the concept of reverse bends (RB) in the MBA unit cell [3]. RBs are usually realized by an off-axis placement of the focusing quadrupole. They help to detach the matching of the dispersion from that of the beta function and significantly reduce the emittance. In 2017, J. Bengtsson and A. Streun adopted the Higher-Order-Achromat approach to MBA-lattices [4,5], where the linear lattice is constructed such, that all 1st and 2nd-order sextupole terms are completely suppressed by phase cancellation.

The BESSY III lattice design intends to integrate all three concepts from the very beginning. To this end, the basic building blocks of MBA lattices, i.e. unit cell (UC), and dispersion suppression cell (DSC) are analysed under the given constraints and with the goals of reaching 100 pm emittance, lowest chromaticity, a momentum compaction factor $\alpha > 10^{-4}$ and a short circumference. It was found, that much orientation in the vast parameter space of lattice design can be gained. By successively stepping though the different options for the design of UC and DSC a baseline version for BESSY III was developed deterministically that fulfills all demands and shows a good non-linear behavior. This approach also puts various commonplace convictions of MBA lattice design into perspective.

CHOICES FOR THE UNIT CELL

The generic, symmetric UC consists of the central dipole, two quadrupoles, QF/RB and QD, and two sextupoles, SF and SD. Drifts are initially set to 0.1 m. The three symmetry conditions $\alpha_{x,y} = \eta' = 0$, are fitted using QF, QD and the RB angle. There are several choices for the UC setup: a) include QD into the main bend (combined function cell, CF-UC) or a separate function cell (SF-UC) b) place the RB or SF at the outside, and, in case of the SF-UC, place QD or SD next to the central dipole. Table 1 lists the emittance, chromaticity and integrated sextupole strength for the six UC options.

Table 1: Features of UC Permutations

UC	Order	ε	ξ_x	ξ_y	SF [1/m²]	SD [1/m²]
CF	SF last	97	-0.7	-0.4	-1.3	1.6
CF	RB last	96	-0.8	-0.3	-2.0	2.2
SF	SF last SD central	94	-0.7	-0.3	-1.0	1.2
SF	RB last SD central	94	-0.8	-0.2	-1.7	1.7
SF	SF last QD central	96	-0.7	-0.3	-1.6	1.8
SF	RB last QD central	97	-0.8	-0.2	-3.5	-3.6

The emittance in all cases is comparable. The critical horizontal chromaticity varies only little, while the sextupole strength varies by more than a factor of 3. The reason lies in the strongly different separation of the beta functions at the location of the sextupoles, see Fig. 1. Interestingly, the length of the CF-UC is close to that of the SF-UC. The bend's gradient reduces the accessible bending field, increasing the dipole length and the stronger sextupoles need additional space. The sextupole strength of a CF-UC lies at least 30 % over the best SF-UC solution, which is chosen for the further analysis.

Effect of the Reverse Bend

The RB has been integrated into the UC from the beginning: without the additional 'knob' of the RB bending field, the UC would increase in length in order to fulfill the symmetry conditions. The deflection angle is ≈ 5 % of the main bend, but needs to be optimized. For a homogeneous dipole, the theoretical minimal emittance, TME, as well as the optimal β_0 and η_0 at the center of the dipole can be calculated [6, 7], using

$$\beta_{0,TME} = \frac{L}{\sqrt{15}}, \quad \eta_{0,TME} = \theta\frac{L}{6}, \quad \varepsilon_{0,TME} \propto \theta^3\frac{2}{3\sqrt{15}},$$

where L denotes half the dipole length and θ half the bending angle. For a main bend of $\theta = 4.5°$, 0.27 m, the TME is 130 pm and is achieved at $\beta_0 = 0.07$ m and $\eta_0 =$

* Work supported by German Bundesministerium für Bildung und Forschung, Land Berlin, and grants of Helmholtz Association
† bettina.kuske@helmholtz-berlin.de

ISBN: 978-3-95450-227-1 ISSN: 2673-5490 doi:10.18429/JACoW-IPAC2022-MOPOTK009

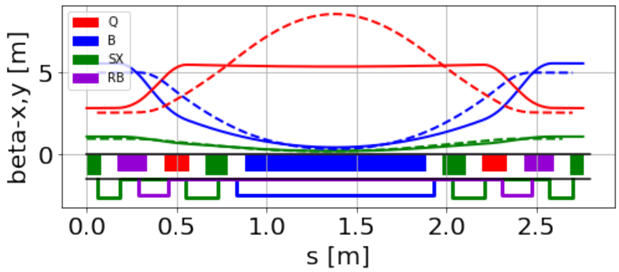

Figure 1: $\beta_{x,y}$, (blue, red) and η (green) in the SF-UC (solid lines, upper structure) and CF-UC (dashed lines, below).

0.002 m, which would obviously demand extremely strong focusing and would create immense chromaticity. Including a RB with an angle of $\theta_{RB} = -0.225°$ (while keeping the total deflection angle) would decrease the TME to 80 pm, for the same values of β_0 and η_0, but still for too large ξ.

Higher Order Achromat (HOA)

The repetitive structure of the UC in MBA lattices suggest to adjust the phase advance between the sextupoles, with the goal to cancel lower orders of the amplitude and momentum dependent tune shifts. The theory [5] translates to the condition $\phi_{x,y} * n = N$ on the phase advance of the UC, where n is the number of UCs used and N is a low integer. Similarly, the phase advance of the full super period should obey $\Phi_{x,y} * p = M$ where p is the periodicity of the ring. These conditions lead to an integer working point of the full lattice, that in the end has to be slightly re-tuned.

The horizontal phase advance in the UC is dominated by the minimum of β_x in the dipole. An upper limit of the total phase advance of the cell can be estimated assuming QD = 0, which leads to a minimal value of β_x in the RB. In this case, β_x propagates like $\beta(s) = \beta_0 + \frac{s^2}{\beta_0}$ between the minimum in the dipole and the RBs and is constant thereafter. The horizontal phase advance of half the unit cell can be approximated by

$$\phi_x = (\arctan(\frac{L_1}{\beta_0}) + \frac{L_2}{\beta_{max}})/2\pi$$

with L1, the length between cell center and the end of RB, and L2, the length between RB and the end.

For values of β_0 from 0.1 m to 0.6 m, the maximum horizontal phase advance varies only little between 0.36 to 0.47. The deflection angle of the dipole has only indirect impact on the phase advance, via the necessary magnet length.

This has significant impact on the lattice setup. Table 2 shows possible combinations of super periods, SP, bends per SP, deflection angle assuming equal dipoles (counting the two half bends in the DSC as one), the phase advance fulfilling the HOA condition and the corresponding β_0 and emittance assuming $\phi_{x,y} * n = 2$.

Table 2 shows, that 5-bend achromats can not be constructed under the taken generic assumptions, as the phase advance can not be reached for the relevant number of SP for BESSY III. Also 7-bend achromats are not attractive due to the larger circumference and increasing emittance. That a larger number of dipoles leads to higher emittance shows the severe impact of imposing the HOA condition. Note that the listed emittance values are only of relative importance, as they do not take the effect of the RB into account.

Table 2: Summary of Lattice Combinations

SP	**bends per SP**	θ [°]	$\phi_x/2\pi$ **HOA**	β_0 **[m]**	ε**[pm]** @$\eta = 0.004$
16	7	3.75	0.33	0.66	271
	6	4.5	0.40	0.40	246
	5	5.625	0.50	-	-
18	7	3.67	0.33	0.64	215
	6	4.0	0.40	0.39	196
	5	5.0	0.50	-	-
20	7	3.0	0.33	0.63	176
	6	3.6	0.40	0.39	162
	5	4.5	0.50	-	-

Ways to Reduce the Emittance

a) Reduction of the Bending Field By increasing the length of the dipole, L, the bending field is reduced below B =1.3 T. The optimal values, $\beta_{0,TME}$, $\eta_{0,TME}$, to achieve minimal emittance, are $\propto L$, while the emittance only depends on θ, the dipole angle. Therefore, longer dipoles relax the focusing in the lattice. The interesting feature of this approach is, that the optical changes are minimal, and the significant gain in emittance is achieved at comparable chromaticity.

Fig. 2 displays the UC's emittance and the chromaticity as a function of the main dipole field. The chromaticity increase over the shown range is small, ≈8 %, for an emittance reduction of 73 %. The increased length of the dipole has the additional benefit of increasing the momentum compaction factor, α_c. At a field of ≈ 0.6 T, $\alpha_c > 2 \times 10^{-4}$ and $\varepsilon < 100$ pm. The related dipole length is 1 m.

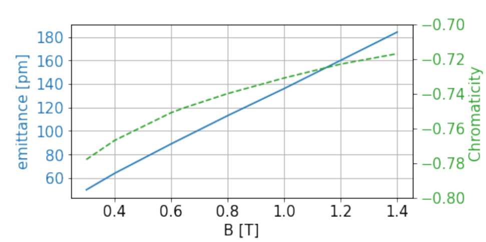

Figure 2: Emittance and chromaticity as a function of the bending field.

b) The Impact of the RB Angle, θ_{RB}, on the emittance results from its contribution to the horizontal damping partition number, J_x. Fig. 3 displays the emittance and J_x as a function of the RB angle. The increase of J_x explains the larger part of the emittance reduction. In addition, larger RB

ISBN: 978-3-95450-227-1 ISSN: 2673-5490 doi:10.18429/JACoW-IPAC2022-MOPOTK009

angles lead to smaller η_0 values, reducing the emittance further. During the variation of θ_{RB}, the transverse optics stays practically unchanged. α_c, though, decreases with larger θ_{RB}, and with lower η_0, limiting the emittance gain.

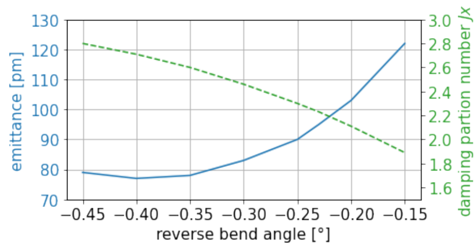

Figure 3: Emittance and the damping partition number, J_x, as a function of the RB angle.

Methods a) and b) result in UCs, where the TME for the dipole conditions can be achieved.

c) Combined Function Bend Fig.4 displays the emittance and J_x as a function of an increasing gradient in the main bend. Unexpectedly, J_x decreases for larger gradients: the contribution of the main dipole to J_x does not change much due to the gradient. The field of QD, though, is lower, leading to a substantially smaller dispersion function at RB, and thus of J_x. The reduction of the damping partition number is reflected in the increasing emittance. The maximal gain in emittance is only a few %. The benefits of a gradient dipole are therefore disputable, when an RB is used.

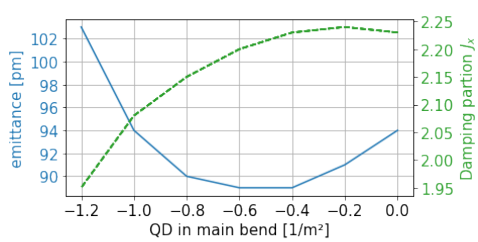

Figure 4: Emittance and damping partition number as a function of a gradient in the main bend.

d) Longitudinal Gradient Bend (LGB) Further emittance reduction can be achieved by splitting the bend longitudinally in several slices. The central slices, where β_x and η_x are small, hold higher fields and the field is lower in the outer slices. In an HOA, β_0 is no 'free' parameter, as it determines the phase advance. η_0 can be adjusted by varying the RB angle. An Emittance of 60 pm can be reached for RB angles of −0.4°, at the cost of α_c turning negative.

DISPERSION SUPPRESSION CELL (DSC)

Two DSCs are located at either end of the repetitive UCs. In the HOA approach, the DSC is as similar as possible to half a UC. DSCs are determined by the boundary conditions set by the UC on one side and the need to suppress the dispersion. Two fit parameters are needed. Principally, there are four options to suppress the dispersion, keeping the homogeneous bend: a) exact setup of the half unit cell, fit with RB and QD; b) RB can be replaced by a pure quadrupole; c) RB can be removed, fit with QD and a drift; d) QD can be removed, fit with RB and a drift. After fitting, the resulting beta functions of the four cases look very similar, QD almost vanishes and if RB is removed, the emittance of the DSC rises by almost 60 %. Therefore, case d) is the best choice, creating space for other needs. Additional dipole length has the same positive effect as in the UC. The β-functions at the end of the DSC dipole have to be matched to $\beta_{x,y} = 2.5$ m and $\alpha_{x,y} = 0$ at the center of the straight section using the 3 quadrupoles and drifts. A gradient in the bend helps to keep the chromaticity of DSC and the straight under control.

BASELINE LATTICE

Fig. 5 displays the resulting baseline lattice. It has an emittance of 101 pm, $\alpha_c = 1.15\,10^{-4}$, a circumference of 357 m and a chromaticity of $\xi_x = -99$ and $\xi_y = -44$. By design, the integrated sextupole strength is weak, SF = 30 m^{-2} and SD = −17 m^{-2}. It is important to notice, that due to the DSC and the straight section there is a significant symmetry break in the phase advance between the sextupoles. It is mandatory to use more than two families of sextupoles to compensate for this, [8]. First tests resulted in a tune shift of $\Delta Q_{x,y} < 0.1$ for an energy deviation of $\Delta p = 3.5$ %. Dynamic apertures where ≈ 3 mm to 4 mm in both planes for a tune shift < 0.1 without harmonic sextupoles or octupoles. This is an excellent starting point for the non-linear optimisation of the lattice.

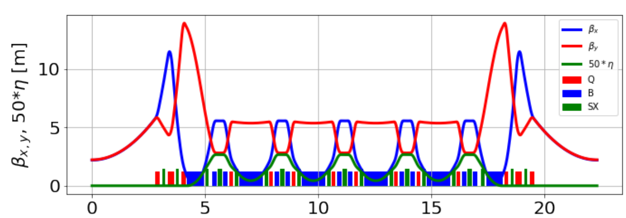

Figure 5: Linear lattice functions emerging from the deterministic approach described in the paper.

CONCLUSION

It has been demonstrated that careful analysis of the different building blocks of MBA lattices leads to a promising lattice candidate without using computer intensive optimisation procedures. Unexpected results were obtained: the commonly applied combined function lattice is not apriori superior to the separated function lattice - the usefulness of a CF magnet can actually be questioned in a lattice with RBs; the emittance can be widely varied without increasing the chromaticity; the most beneficial knob is the dipole length, as it decreases the emittance while increasing α_c; longitudinal gradient bends are associated with a significant reduction of α_c down to negative values. The baseline lattice is now subject to further non-linear and technical optimization.

ISBN: 978-3-95450-227-1 ISSN: 2673-5490 doi:10.18429/JACoW-IPAC2022-MOPOTK009

REFERENCES

[1] P. Goslawski et al., “BESSY III Status Report and Overview”, presented at the 13th Int. Particle Accelerator Conf. (IPAC’22), Bangkok, Thailand, Jun. 2022, paper TUPOMS010, unpublished.

[2] S. Leemann, M. Eriksson, et al, "‘Beam dynamics and expected performance of Sweden’s new storage-ring light source: MAX IV"’, *Phys. Rev. ST Accel. Beams*, vol. 12, 2009. doi:10.1103/PhysRevSTAB.12.120701

[3] A. Streun, "‘The Anti-Bend Cell for Ultralow Emittance Storage Ring Lattices"’, *Nucl. Inst. Meth.* A, vol. 737, 2014. *doi:10.1016/j.nima.2013.11.064*

[4] J. Bengtsson, A. Streun, "Robust Design Strategy for SLS-2", Paul Scherrer Institute, Villingen, Switzerland, SLS2-BJ84-001-2, June 2017.

[5] J. Bengtsson, "The Sextupole Scheme for the Swiss Light Source (SLS): An Analytical Approach", Paul Scherrer Institute, Villingen, Switzerland, SLS note 9-97, Mar. 1997.

[6] L. C. Teng, "Minimum Emittance Lattice for Sychrotron Radiation Storage Rings", Argonne National Laboratory Technical Report No. LS-17, 1985

[7] B. Riemann, A. Streun, “Low Emittance Lattice Design from first Principles: Reverse Bending and Longitudinal Gradient Bends”, *Phys. Rev. Accel. Beams* 22, 021601 (2019). doi:10.1103/PhysRevAccelBeams.22.021601

[8] J. Bengtsson, M. Abo-Bakr, P. Goslawski, A. Jankowiak, and B. C. Kuske, “Robust Design and Control of the Nonlinear Dynamics for BESSY-III”, presented at the 13th Int. Particle Accelerator Conf. (IPAC’22), Bangkok, Thailand, Jun. 2022, paper THPOPT051, unpublished.